

Comprehensive Monosynaptic Rabies Virus Mapping of Host Connectivity with Neural Progenitor Grafts after Spinal Cord Injury

Andrew F. Adler,¹ Corinne Lee-Kubli,¹ Hiromi Kumamaru,¹ Ken Kadoya,^{1,3} and Mark H. Tuszynski^{1,2,*}

¹Department of Neurosciences, University of California – San Diego, La Jolla, CA 92093, USA

²Veterans Administration San Diego Healthcare System, San Diego, CA 92161, USA

³Present address: Department of Orthopaedic Surgery, Hokkaido University, Sapporo 060-8638, Japan

*Correspondence: mtuszynski@ucsd.edu

<http://dx.doi.org/10.1016/j.stemcr.2017.04.004>

SUMMARY

Neural progenitor cells grafted to sites of spinal cord injury have supported electrophysiological and functional recovery in several studies. Mechanisms associated with graft-related improvements in outcome appear dependent on functional synaptic integration of graft and host systems, although the extent and diversity of synaptic integration of grafts with hosts are unknown. Using transgenic mouse spinal neural progenitor cell grafts expressing the TVA and G-protein components of the modified rabies virus system, we initiated monosynaptic tracing strictly from graft neurons placed in sites of cervical spinal cord injury. We find that graft neurons receive synaptic inputs from virtually every known host system that normally innervates the spinal cord, including numerous cortical, brainstem, spinal cord, and dorsal root ganglia inputs. Thus, implanted neural progenitor cells receive an extensive range of host neural inputs to the injury site, potentially enabling functional restoration across multiple systems.

INTRODUCTION

Recent reports demonstrate the ability of neural stem cell (NSC) and neural progenitor cell (NPC) grafts to integrate into sites of spinal cord injury (SCI) and improve motor outcomes (Bonner et al., 2011; Kadoya et al., 2016; Lu et al., 2012, 2014; Rossi et al., 2010). For example, rats with complete thoracic spinal cord transection recover hindlimb movements after NPC grafting, and re-transection of the spinal cord above the graft abolishes activity, suggesting that host-to-graft-to-host connectivity is associated with recovery (Lu et al., 2012). Anatomical tracing of axonal projections into grafts indicates that host corticospinal (Kadoya et al., 2016), raphespinal (Lu et al., 2012), and sensory (Bonner et al., 2011) systems regenerate into grafts at sites of SCI. In some cases, synaptic connectivity between host and graft has been confirmed by electron microscopy and electrophysiology (Kadoya et al., 2016; Lu et al., 2012, 2014).

While informative, the preceding studies have sampled isolated host inputs into grafts, leaving us lacking an appreciation of the full spectrum of host-graft connectivity. How extensively can host neurons synapse with graft neurons in the injured spinal cord? Skilled motor functions such as dexterous forelimb control require integration across corticospinal, rubrospinal, reticulospinal, and propriospinal systems (Azim et al., 2014; Esposito et al., 2014), and regeneration of several or all of these motor systems may be necessary to support functional recovery. Similarly, recovery of sensory function may only be possible if sensory axons innervate NPC grafts. If only a subset of host systems form synaptic contacts with grafts, functional outcomes may be limited. Moreover, the mere presence of a host

axon in an NPC graft does not confirm that a host-to-graft synaptic connection has actually been formed.

To evaluate the potential of NPC grafts to interact with a variety of host axonal systems, we employed a rabies virus tool to comprehensively map monosynaptic host inputs into grafts placed in sites of SCI. We used a modified rabies virus expressing mCherry, wherein the virus: (1) was EnvA pseudotyped, such that it depends on expression of TVA (receptor of the avian sarcoma leucosis virus subgroup A) for initial infection of cells, and (2) was rabies glycoprotein (G-protein) deleted, rendering the rabies incapable of transsynaptic transport unless an infected cell also expressed rabies G-protein. This EnvA-pseudotyped, G-deleted-mCherry rabies virus (EnvA-SADΔG-mCherry) induces strong expression of mCherry in cells expressing the TVA receptor and G-protein, as well as in their immediate presynaptic partners (Osakada and Callaway, 2013). Using this tool, we now find that grafts of NPCs to sites of mouse SCI receive synaptic connectivity from all major host systems that normally project to the intact spinal cord.

RESULTS

As noted above, our goal was to initiate monosynaptically restricted mCherry rabies virus infection exclusively from grafted neurons placed in SCI lesion sites. In this case, any host neurons that are labeled with mCherry have made monosynaptic contact onto graft neurons. To produce donor NPCs that could be infected with EnvA-SADΔG-mCherry, we crossed mice that express the



Rabies-Helper Grafts

Wild-Type Grafts (Controls)

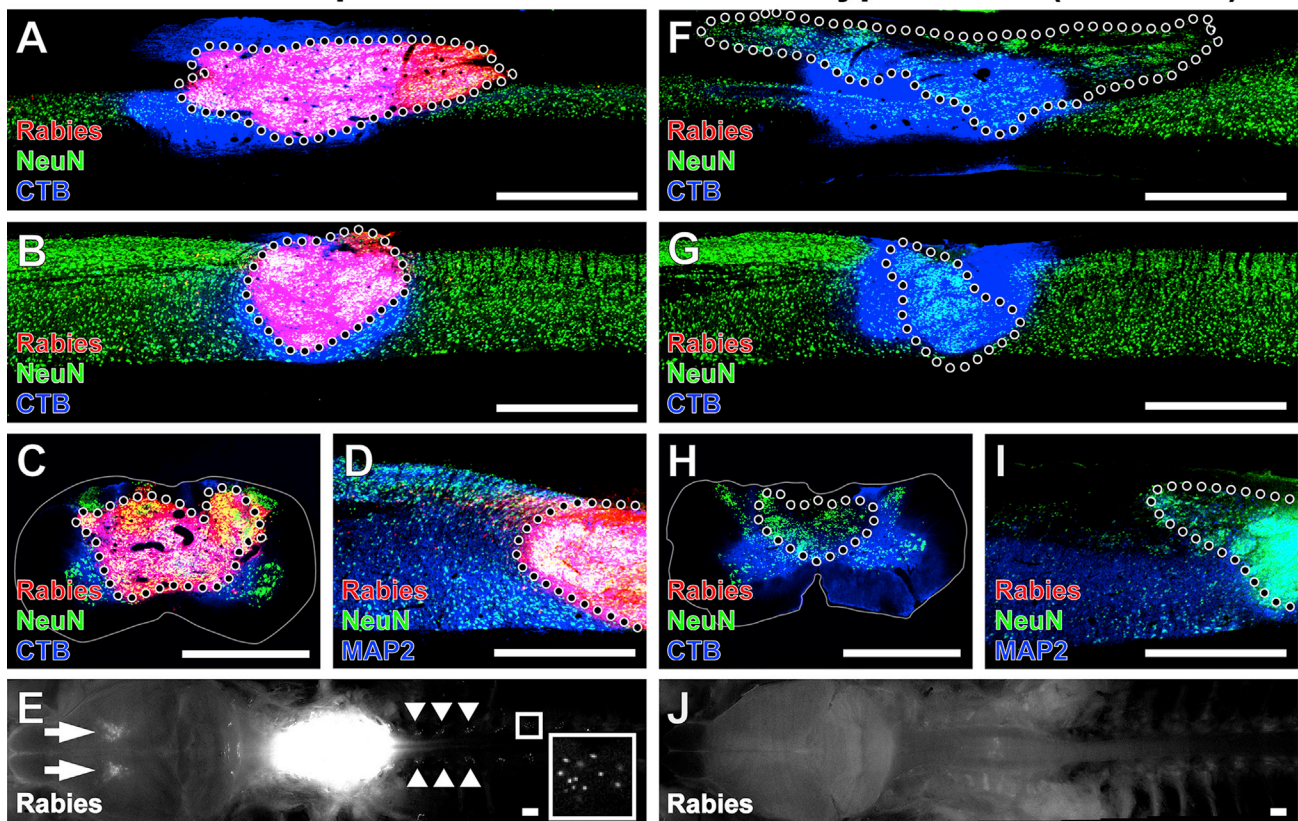


Figure 1. Monosynaptically Restricted Rabies Infection Initiated Exclusively from Rabies-Helper Spinal NPC Grafts after SCI

Grafts of either (A–E) Rabies-Helper-expressing NPC grafts or (F–J) Wild-Type grafts lacking rabies-helper components.

(A) Sagittal view near the central canal of a Rabies-Helper NPC graft in a C4 spinal cord lesion site 3 months after lesion/grafting and 1 week after EnvA-SADΔG-mCherry rabies virus (red) injection into graft. CTB (blue) co-injected with rabies diffuses beyond the graft, whereas mCherry expression is strictly initiated from graft neurons. NeuN, green. Rostral is to the left, caudal to the right.

(B) Sagittal view through a more lateral section of a Rabies-Helper NPC graft, showing the extent of injury to host gray matter.

(C) Transverse view of a Rabies-Helper graft in a second animal, showing that the lesion extends to involve some of the lateral and ventral white matter.

(D) Sagittal view of MAP2 (blue) and NeuN (green) expression in graft neurons.

(E) Gross horizontal view of brain/brainstem/spinal cord preparation, showing intense expression of Rabies-mCherry under fluorescent illumination in the graft at the lesion site (white, center of image) and retrograde transsynaptic expression of Rabies-mCherry in the cortex (arrows) and in several dorsal root ganglia (arrowheads). A sample DRG is shown at higher magnification in the inset.

(F–J) In animals that received Wild-Type grafts followed by injections of SADΔG-mCherry rabies virus and CTB, there is not a single cell expressing Rabies-mCherry in the graft (F–I) or at remote host locations (J).

Scale bars, 1 mm. Dotted lines denote graft-host borders. Solid lines denote the extent of white matter in transverse sections. See also Figure S1.

rabies-helper components (TVA/G-protein) in a Cre-dependent fashion with Synapsin-Cre mice, enabling constitutive neuronal expression of rabies helper in neurons of progeny (referred to as Rabies-Helper mice). Control (Wild-Type) grafts consisted of wild-type NPCs (entirely lacking TVA/G-protein expression).

Donor NPCs for grafting to sites of SCI were obtained from embryonic day 12.5–13.5 (E12.5–E13.5) spinal cords

of Rabies-Helper or wild-type (control) embryos. Cells were harvested, suspended in PBS, and immediately grafted into C4 spinal cord lesions in adult athymic (nude) mice (which lack TVA/G-protein). C4 spinal cord dorsal lesions were placed immediately prior to grafting using a Scouten wire knife that removed the dorsal columns and extensive regions of central gray matter (Figures 1 and S1) but left overlying dura intact.



EnvA-SADΔG-mCherry rabies virus was injected 1–3 months after injury/grafts into a total of eight sites in Rabies-Helper grafts ($n = 8$ animals). Animals were killed 1 week later. Only graft-derived neurons from Rabies-Helper grafts should be capable of being primarily infected by the pseudotyped rabies virus. To confirm the exclusivity of initial rabies infection to Rabies-Helper grafts, three negative control animals received Wild-Type grafts that did *not* express TVA/G-protein, and also received EnvA-SADΔG rabies virus injections. For all animals traced at 3 months, we co-injected the conventional (non-transsynaptic) retrograde tracer cholera toxin subunit B (CTB) with the rabies virus to assess the comparability of injections between animals.

As a positive control, we co-injected *adult* Rabies-Helper mice bilaterally throughout gray matter at C4 with EnvA-SADΔG-mCherry rabies and CTB ($n = 3$). In these intact animals, rabies traveled polysynaptically from the injection sites. Raw counts of Rabies-mCherry⁺ and CTB⁺ neurons used for supraspinal quantifications are provided in Table S1.

EnvA-SADΔG-mCherry Rabies Virus Infectivity Is Specific to NPC Grafts Expressing Rabies-Helper Components

NPC grafts survived and filled the lesion sites in all animals, and differentiated into MAP2⁺NeuN⁺ neurons (Figures 1 and S1). In animals that received EnvA-SADΔG-mCherry rabies virus injections into Wild-Type grafts lacking TVA and G-protein, there was a total absence of Rabies-mCherry expression in any graft or host cell (Figures 1F–1J and S1–S4). In contrast, all Rabies-Helper spinal cord NPC grafts were robustly infected with Rabies-mCherry throughout grafts, with an average of 47% of NeuN⁺ graft neurons expressing Rabies-mCherry (Figure S1B). Thus, EnvA-pseudotyped rabies infection reliably depended upon expression of TVA/G-protein within grafts, highlighting the accuracy of host tracing in animals that received Rabies-Helper grafts. Retrograde spread of CTB from control graft sites to supraspinal nuclei was similar to the spread from Rabies-Helper graft sites (Figures 2, 3, S2, and S3), demonstrating comparable injection technique between control and experimental animals. In addition to Rabies-Helper graft infection with Rabies-mCherry, numerous host neurons in multiple spinal cord and brain regions expressed Rabies-mCherry (Figures 1, 2, 3, 4, and S4), indicating monosynaptic retrograde transport to the host.

Cortical Connectivity with Grafts

Retrograde Rabies-mCherry virus expression was present in regions of the cortex known to give rise to corticospinal projections (Figures 1E and 2). Indeed, Rabies-mCherry labeling was so intense that the apical dendrites of corticospinal tract (CST) neurons were grossly visible (Figures 1E

and 2A). The greatest concentration of labeled CST neurons was located in the primary motor cortex (M1, Figures 2A–2C), a pattern that was consistent among all Rabies-Helper-grafted animals (Figure S4). Fibers arising from M1 constitute the most abundant component of the intact cortical projection to the cervical spinal cord (Liang et al., 2011). Projections from the primary somatosensory cortex contained the second highest proportion of cortical synaptic connections with grafts (Figures 2C and 2D). Projections from M2 (premotor cortex) were also frequent (Figures 2C and 2D), whereas projections from secondary somatosensory cortex to grafts were comparatively rare (Figure 2C), as they are in the intact system (Liang et al., 2011). In mice, these cortical areas caudal to bregma elicit a mixture of forelimb and hindlimb movements, and have been implicated in spontaneous motor map recovery after dorsal column lesions at cervical levels via sprouting of the CST (Hilton et al., 2016; Hollis et al., 2016).

Subcortical Connectivity with Grafts

Neurons were labeled for Rabies-mCherry in the red nucleus, indicating that they formed monosynaptic projections into grafts (Figure 2E). Together with the corticospinal projection, rubrospinal projections influence skilled forelimb function in rodents (Deumens et al., 2005), and are known to sprout in response to SCI (Takeoka et al., 2014).

Numerous reticular nuclei with known projections to the spinal cord also contained Rabies-mCherry⁺ neurons (Figures 3A, 3B, and 3D), constituting the most abundant supraspinal projection to the NPC grafts (27% of all labeled supraspinal neurons, Figures 3L and 3M). The reticular nuclei include several subdivisions, including the gigantocellular (Gi) and medullary reticular formation nuclei. Neurons in Gi exhibit structural plasticity and have been implicated in functional recovery after SCI (Takeoka et al., 2014; Zörner et al., 2014). Neurons in the ventral part of the medullary reticular nucleus (MdV) receive CST and rubral input, and project to cervical forelimb motor pools, where they contribute to skilled forelimb reaching (Esposito et al., 2014). In addition, Rabies-mCherry⁺ neurons were present in the spinal trigeminal and solitary nuclei (Figures 3C and 3E). The solitary nucleus receives visceral sensory information to regulate respiration via projections to phrenic motor neurons in the cervical spinal cord (Liang et al., 2011).

Rabies-mCherry⁺ neurons were also present in caudal raphe nuclei, comprising 3% of supraspinal projections into grafts (Figures 3G, 3H, and 3L). 5-HT-labeled axons were observed penetrating grafts (Figure 3I). Spinal projection neurons in the caudal raphe make monosynaptic contact with motor neurons, and mediate rhythmic locomotor activity (Deumens et al., 2005) and nociceptive pain perception in the intact spinal cord (Liang et al., 2011). 5-HT-immunoreactive cell bodies were not present in grafts.

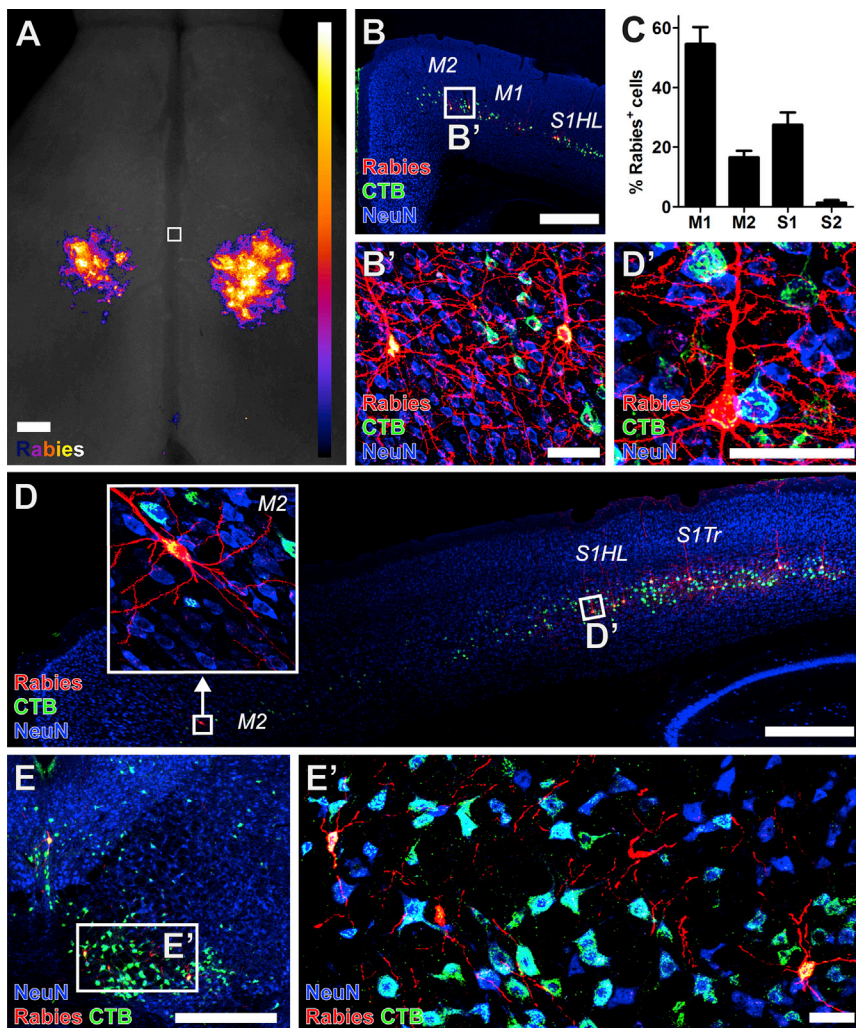


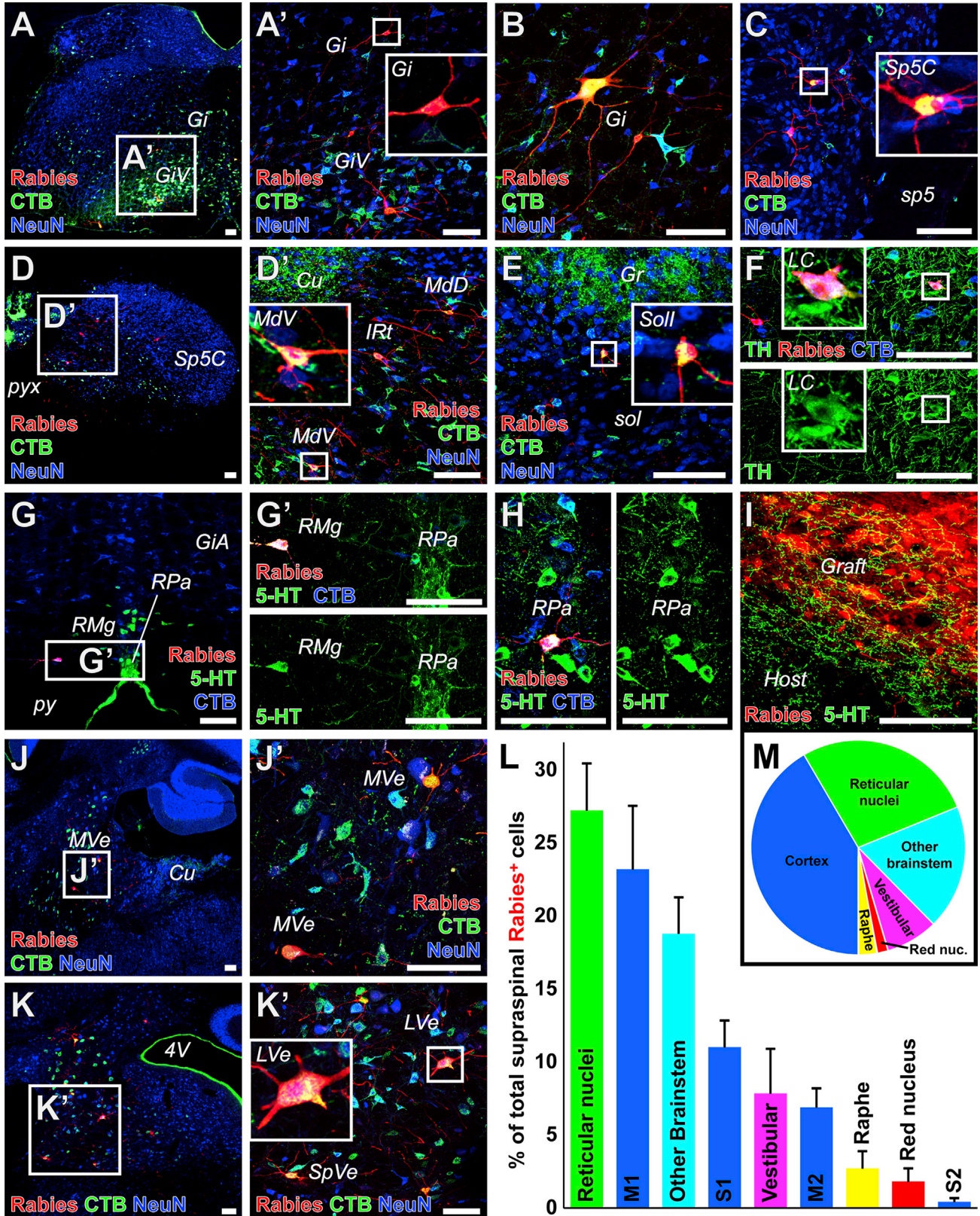
Figure 2. Host Cortical and Rubral Neurons Make Monosynaptic Contact with Graft Neurons

(A) Heatmap of the location of Rabies-mCherry⁺ corticospinal neurons making monosynaptic contact onto Rabies-Helper spinal NPC graft-derived neurons (aggregate of $n = 8$ mice). Horizontal view. Square denotes bregma, with rostral at the top of the image. Most of the Rabies-mCherry signals from the apical dendrites of corticospinal neurons are located caudal to the bregma, in the caudal forelimb and hindlimb regions. (B and C) Rabies-mCherry⁺ (red) cortical neurons making synaptic contacts onto graft neurons co-labeled with CTB injected into graft sites (green), and were (C) found most frequently in the primary motor cortex (M1; mean of all Rabies-Helper grafted mice cut coronally, \pm SEM, $n = 5$). NeuN, blue. (D) Rabies-mCherry⁺ cortical neurons making synaptic contacts onto graft neurons were also found in the secondary motor cortex (M2, boxed detail) in the rostral forelimb area, and hindlimb and trunk primary somatosensory cortex (S1HL, S1Tr). (E) Rabies-mCherry⁺ neurons were also present in the red nucleus. 30- μ m-thick sections. Scale bars, 500 μ m in (A, B, D, and E) and 50 μ m in (B', D', and E'). See also Figures S2 and S4.

Occasional Rabies-mCherry⁺ neurons were also present in the locus coeruleus. These neurons co-labeled with tyrosine hydroxylase (TH) and CTB, confirming their identity as cerulospinal neurons (Figure 3F). The locus coeruleus contains TH⁺ norepinephrinergic cells with projections to the spinal cord ventral and dorsal gray matter, regulating muscle tone and pain sensation, respectively (Samuels and Szabadi, 2008).

Finally, Rabies-mCherry⁺ neurons were present in several vestibular nuclei with spinal projections, including the medial, spinal, and lateral vestibular nuclei (MVe, SpVe, and LVe; Figures 3J and 3K). Collectively, vestibulospinal projections constituted 8% of supraspinal projections to the graft (Figures 3L and 3M). Vestibulospinal neurons make monosynaptic contacts onto premotor spinal interneurons (Bourane et al., 2015), and the lateral vestibular nucleus (LVe) innervates motor neurons at lumbar levels of the spinal cord (Basaldella et al., 2015).

Thus, all known major brainstem projections to the intact spinal cord also connected with graft neurons, in proportions that generally reflect the relative weight of inputs to the intact cervical spinal cord (Liang et al., 2011). *Spinal Interneuron Connectivity with Grafts* Rabies-mCherry labeled descending and ascending propriospinal neurons rostral and caudal to the grafting site, at cervical through lumbar levels (Figures 4A–4C). Spinal interneurons projecting into grafts from C2 included CHX10⁺ and SATB1⁺ interneurons (Figures 4D and 4E), marking populations of premotor neurons that receive cortical inputs (Azim et al., 2014; Levine et al., 2014). In addition, occasional Rabies-mCherry⁺ChAT⁺ V0c interneurons were observed near the central canal (Figure 4F). Of all host CNS neurons synapsing with grafts, connections from spinal interneurons were the most abundant, qualitatively constituting approximately 50% of input to grafts.



(legend on next page)



Dorsal Root Ganglia Connectivity with Grafts

Numerous DRG neurons formed monosynaptic projections into grafts, as demonstrated by Rabies-mCherry⁺ DRG neurons at multiple spinal levels (Figures 4G–4L). DRGs with the highest number of labeled neurons were present at C6 (two spinal segments caudal to grafts) and adjacent segments, with few DRG neurons labeled at lumbar levels (Figures 4G and 4H). Host DRG neurons projecting into grafts included large-diameter neurofilament 200 and CALRETININ-expressing neurons (Figures 4I and 4J), marking proprioceptors and sensory neurons responsive to touch (Bourane et al., 2015), and small-diameter calcitonin gene-related peptide-expressing and isolectin B4-binding nociceptive neurons (Figures 4K and 4L).

Connectivity in Intact Spinal Cords

Using pseudotyped rabies virus, we compared monosynaptic host inputs to grafts, to polysynaptic inputs to the intact spinal cord. Intact adult Rabies-Helper mice received injections of the same amount of rabies and CTB that was injected into grafted animals throughout the gray matter at C4. Rabies labeling in Rabies-Helper mice proceeds polysynaptically because, in this case, all neurons express TVA and G-protein. Animals were killed 7 days after injection, and exhibited extensive mCherry labeling in nuclei with spinal projections (Figures S2E, S3H, and S3I). Rabies-mCherry was also observed in neurons that polysynaptically project to the spinal cord, including cerebellar Purkinje neurons (Figure S2F). Purkinje neurons were never Rabies-mCherry⁺ in Rabies-Helper grafted animals, providing confirmation of monosynaptically restricted tracing in these mice. Like monosynaptically traced animals receiving Rabies-Helper grafts, polysynaptic intact Rabies-Helper animals had greater numbers of CTB-labeled cortical neurons compared with Rabies-mCherry⁺ neurons (Figure S2E and Table S1), suggesting either greater spread or uptake of CTB from injection sites compared with rabies.

DISCUSSION

We have used a monosynaptically restricted retrograde rabies virus vector to assess the connectivity of NPC grafts in the injured spinal cord. We find that every major functional system exhibits synaptic connectivity with grafts, including cortical, brainstem, intraspinal, and sensory systems. Thus, the potential exists for NPC/NSC grafts to simultaneously impact a variety of functional motor and sensory outcomes after SCI.

In using the EnvA-SADΔG rabies virus tool to comprehensively map host projections into NPC grafts, the benefits and limitations of the approach need to be considered. One primary benefit is the ability to genetically initiate labeling from the graft exclusively, reducing or eliminating the possibility of artefactual labeling by unintentional spread of a conventional retrograde tracer into host tissue, when the intention is to solely inject the graft. Another benefit is the ability to simultaneously sample a very broad diversity of host inputs into grafts; indeed, one may be able to detect virtually all modalities of host inputs to grafts. Individual circuits of the spinal cord have been studied in thousands of reports spanning the last 100 years, but rabies tracing enables comprehensive mapping of potentially all types of host inputs into NPC grafts in a single study, or even in a single animal. However, there may be biases in the efficiency of rabies labeling across different types of synapses: for example, SADΔG rabies virus may generally label short-distance projections more efficiently than long-distance projections (Reardon et al., 2016). Thus, although graft-initiated EnvA-SADΔG rabies tracing can unambiguously elucidate populations of host neurons that synapse with graft neurons, it is insufficient to demonstrate an absence of synaptic input from a particular host region; in the present study, this point is moot since all major spinal projections to the intact spinal cord were identified to project into grafts. However, the

Figure 3. Host Brainstem Neurons Make Monosynaptic Contact with Graft Neurons

(A–H) Host Rabies-mCherry⁺ (red) neurons making monosynaptic contact onto Rabies-Helper graft neurons co-labeled with CTB injected into graft sites were found in (A and B) the gigantocellular (Gi) and gigantocellular, ventral part (GiV) reticular nuclei, (C) the caudal part of the spinal trigeminal nucleus (Sp5C) adjacent to the spinal trigeminal tract (sp5), (D) the ventral/intermediate/dorsal parts of the medullary reticular nucleus (MdV/IRt/MdD) adjacent to the cuneate nucleus (Cu) and pyramidal decussation (pyx), and (E) the interstitial part of the nucleus of the solitary tract (SolI) adjacent to the solitary tract (sol) and gracile nucleus (Gr). Host mCherry⁺CTB⁺ neurons making monosynaptic contact with graft neurons were also co-labeled with tyrosine hydroxylase (TH, green) in the locus coeruleus (LC) (F), and in the raphe magnus (RMg) (G), and the raphe pallidus (RPa) (H) co-labeled with serotonin (5-HT, green) adjacent to the pyramidal tracts (py) and alpha part of the gigantocellular reticular nucleus (GiA).

(I) Serotonergic host axons penetrated grafts.

(J and K) Host mCherry⁺CTB⁺ neurons making monosynaptic contact with graft neurons were also found in the medial vestibular nucleus (MVe) adjacent to cuneate nucleus (Cu) (J), and in the lateral and spinal vestibular nuclei (LVe, SpVe) adjacent to the fourth ventricle (4V) (K).

(L) Among all supraspinal Rabies-mCherry⁺ neurons, those found in reticular and corticospinal nuclei were the most common (mean ± SEM of all Rabies-Helper-grafted mice cut transversely, n = 5).

(M) Pie chart representation of data in (L). Insets depict detail of boxed regions. Transverse sections, except sagittal in (J and J'). 30-μm-thick sections. Scale bars, 100 μm. See also Figure S3.

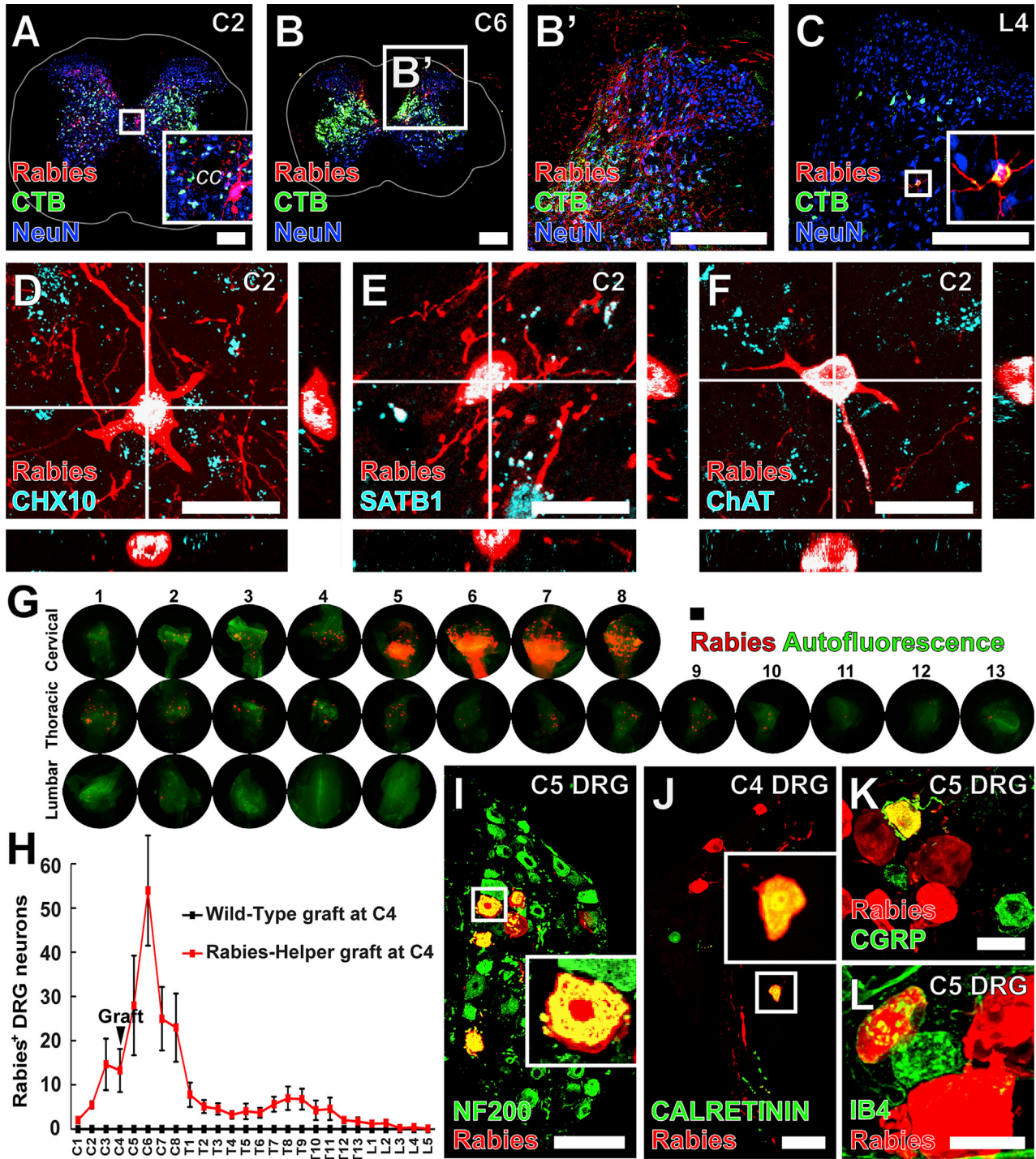


Figure 4. Host Spinal and Dorsal Root Ganglia Neurons Make Monosynaptic Contact with Graft-Derived Neurons

(A–C) Host Rabies-mCherry⁺ (red) neurons making monosynaptic contact with Rabies-Helper graft neurons co-labeled with CTB (green) injected into graft sites were found in the cervical spinal cord rostral (A) and caudal (B) to graft sites, as well as less frequently at lumbar levels (transverse sections) (C). White lines denote the extent of white matter.

(D and E) At C2, Rabies-mCherry⁺CHX10⁺ (D), and Rabies-mCherry⁺SATB1⁺ neurons (E) were present in the intermediate gray matter where premotor CHX10⁺ V2a and SATB1/2⁺ interneurons are located.

(legend continued on next page)



number of rabies-labeled host neurons is likely an underestimate of the true number of host-graft connections formed. Future work will determine which of these host inputs to grafts mediate functional improvement after SCI (Kadoya et al., 2016; Lu et al., 2012).

While this study employs the EnvA-SADΔG rabies virus to map host connectivity with an NPC graft in an SCI model, a previous study used EnvA-SADΔG rabies virus to map the connections of a neural graft implanted into a phototoxic cell loss model in the visual cortex: implanted cells received appropriate synaptic inputs from host neurons that normally project to the graft site (Falkner et al., 2016). The latter findings indicated that host systems retain an ability to recognize cues in NSCs to recapitulate appropriate connections. Another study used *pseudorabies* virus (as distinct from *pseudotyped* rabies virus) to approximate host connectivity to an NSC graft in a model of SCI (Lee et al., 2014), but in this case infection could be initiated from host neurons, as well as travel across multiple host-host synapses; therefore monosynaptic host inputs to the graft could not be determined.

Overall, our study provides a comprehensive map of host inputs into an NPC graft placed in a site of SCI, revealing the host-graft connectome. The broad host inputs from every major motor and sensory functional system suggest the ability of NPC grafts to influence several functional domains that are lost after SCI. The efficiency of the EnvA-SADΔG rabies tool substantially exceeds that of anterograde tracing techniques initiated from the host and the reliability of conventional retrograde tracers injected into grafts, and confirms the presence of host-graft synapses. This tool could also be used in future studies to initiate labeling from the host rostral or caudal to the injury site, retrogradely to the graft, thereby assessing graft-to-host connectivity.

EXPERIMENTAL PROCEDURES

Research Animals and Ethical Permissions

In total, 45 mice were used. Procedures were performed in accordance with The NIH Guide for the Care and Use of Laboratory Animals, and were approved by the Veterans Affairs San Diego

Healthcare System IACUC. Details of breeding, SCI, and grafting are provided in [Supplemental Experimental Procedures](#).

EnvA-SADΔG-mCherry Rabies Virus Injections

Grafts or intact animals were injected with 1.5 μL of 1×10^7 vg/mL EnvA-SADΔG-mCherry rabies virus in Hank's balanced salt solution (HBSS). Grafts at 3 months of maturation were co-injected with rabies virus and 0.2% CTB in HBSS. Details are provided in [Supplemental Experimental Procedures](#).

Immunofluorescence and Microscopy

Samples were fixed in 4% paraformaldehyde. Images of stained sections were captured with either Olympus AX70 (widefield) or FV-1000 (confocal) microscopes. Details of antibodies and dilutions are provided in [Supplemental Experimental Procedures](#).

SUPPLEMENTAL INFORMATION

Supplemental Information includes Supplemental Experimental Procedures, four figures, and one table and can be found with this article online at <http://dx.doi.org/10.1016/j.stemcr.2017.04.004>.

AUTHOR CONTRIBUTIONS

A.F.A., C.L.K., K.K., and M.H.T. designed the study. A.F.A. and C.L.K. performed SCI and Rabies-Helper/wild-type spinal NPC grafting surgeries. A.F.A. performed rabies/CTB injection surgeries. A.F.A. and C.L.K. immunolabeled and imaged CNS/PNS tissue. H.K. immunolabeled and imaged spinal interneuron subtypes. A.F.A. and M.H.T. wrote the manuscript.

ACKNOWLEDGMENTS

We thank E. Staufenberg, B. Durham, S. Im, G. Poplawski, J. Dulin, L. Graham, J. Weber, S. Ceto, J. Connor, P. Lu, and D. Gibbs for technical assistance. This work was supported by the Veterans Administration (Gordon Mansfield Spinal Cord Injury Consortium), the Craig H. Neilsen Foundation, the Bernard and Anne Spitzer Charitable Trust, the Dr. Miriam and Sheldon G. Adelson Medical Research Foundation, Grants-in-Aid for Scientific Research, and the Japan Society for the Promotion of Science.

Received: January 7, 2017

Revised: April 4, 2017

Accepted: April 5, 2017

Published: May 4, 2017

(F) Rabies-mCherry⁺ChAT⁺ neurons were also found adjacent to the central canal (cc), where premotor V0c ChAT⁺ neurons are located. Transverse sections.

(G) Rabies-mCherry⁺ DRG neurons making monosynaptic contact with graft neurons were found at cervical, thoracic, and lumbar levels, both rostral and caudal to the injury and graft site.

(H) Most labeled DRG neurons were found at cervical levels immediately caudal to the graft site (mean ± SEM, n = 8 Rabies-Helper grafted mice, n = 3 Wild-Type grafted mice).

(I–L) Some large-diameter Rabies-mCherry⁺ DRG neurons expressed (I) neurofilament 200 (NF200) or (J) CALRETININ, and some small-diameter Rabies-mCherry⁺ DRG neurons (K) expressed calcitonin gene-related peptide (CGRP), or (L) bound isolectin B4 (IB4), marking sensory neurons responsive to (I and J) touch and (K and L) noxious stimuli. Insets depict detail of boxed regions.

30-μm-thick sections for (A–F), 20-μm-thick sections for (I–K). Scale bars, 250 μm in (A–C), 20 μm in (D–F), 100 μm in (G, I, and J), and 30 μm in (K and L). See also [Figure S3](#).



REFERENCES

- Azim, E., Jiang, J., Alstermark, B., and Jessell, T.M. (2014). Skilled reaching relies on a V2a propriospinal internal copy circuit. *Nature* 508, 357–363.
- Basaldella, E., Takeoka, A., Sigrist, M., and Arber, S. (2015). Multi-sensory signaling shapes vestibulo-motor circuit specificity. *Cell* 163, 301–312.
- Bonner, J.F., Connors, T.M., Silverman, W.F., Kowalski, D.P., Lemay, M.A., and Fischer, I. (2011). Grafted neural progenitors integrate and restore synaptic connectivity across the injured spinal cord. *J. Neurosci.* 31, 4675–4686.
- Bourane, S., Grossmann, K.S., Britz, O., Dalet, A., Del Barrio, M.G., Stam, F.J., Garcia-Campmany, L., Koch, S., and Goulding, M. (2015). Identification of a spinal circuit for light touch and fine motor control. *Cell* 160, 503–515.
- Deumens, R., Koopmans, G.C., and Joosten, E.A. (2005). Regeneration of descending axon tracts after spinal cord injury. *Prog. Neurobiol.* 77, 57–89.
- Esposito, M.S., Capelli, P., and Arber, S. (2014). Brainstem nucleus MdV mediates skilled forelimb motor tasks. *Nature* 508, 351–356.
- Falkner, S., Grade, S., Dimou, L., Conzelmann, K.-K., Bonhoeffer, T., Götz, M., and Hübener, M. (2016). Transplanted embryonic neurons integrate into adult neocortical circuits. *Nature* 539, 248–253.
- Hilton, B.J., Anenberg, E., Harrison, T.C., Boyd, J.D., Murphy, T.H., and Tetzlaff, W. (2016). Re-establishment of cortical motor output maps and spontaneous functional recovery via spared dorsolaterally projecting corticospinal neurons after dorsal column spinal cord injury in adult mice. *J. Neurosci.* 36, 4080–4092.
- Hollis, E.R., II, Ishiko, N., Yu, T., Lu, C.-C., Haimovich, A., Tolentino, K., Richman, A., Tury, A., Wang, S.-H., and Pessian, M. (2016). Ryk controls remapping of motor cortex during functional recovery after spinal cord injury. *Nat. Neurosci.* 19, 697–705.
- Kadoya, K., Lu, P., Nguyen, K., Lee-Kubli, C., Kumamaru, H., Yao, L., Knackert, J., Poplawski, G., Dulin, J.N., and Strobl, H. (2016). Spinal cord reconstitution with homologous neural grafts enables robust corticospinal regeneration. *Nat. Med.* 22, 479–487.
- Lee, K.-Z., Lane, M.A., Dougherty, B.J., Mercier, L.M., Sandhu, M.S., Sanchez, J.C., Reier, P.J., and Fuller, D.D. (2014). Intraspinal transplantation and modulation of donor neuron electrophysiological activity. *Exp. Neurol.* 251, 47–57.
- Levine, A.J., Hinckley, C.A., Hilde, K.L., Driscoll, S.P., Poon, T.H., Montgomery, J.M., and Pfaff, S.L. (2014). Identification of a cellular node for motor control pathways. *Nat. Neurosci.* 17, 586–593.
- Liang, H., Paxinos, G., and Watson, C. (2011). Projections from the brain to the spinal cord in the mouse. *Brain Struct. Funct.* 215, 159–186.
- Lu, P., Wang, Y., Graham, L., McHale, K., Gao, M., Wu, D., Brock, J., Blesch, A., Rosenzweig, E.S., and Havton, L.A. (2012). Long-distance growth and connectivity of neural stem cells after severe spinal cord injury. *Cell* 150, 1264–1273.
- Lu, P., Woodruff, G., Wang, Y., Graham, L., Hunt, M., Wu, D., Boehle, E., Ahmad, R., Poplawski, G., and Brock, J. (2014). Long-distance axonal growth from human induced pluripotent stem cells after spinal cord injury. *Neuron* 83, 789–796.
- Osakada, F., and Callaway, E.M. (2013). Design and generation of recombinant rabies virus vectors. *Nat. Protoc.* 8, 1583–1601.
- Reardon, T.R., Murray, A.J., Turi, G.F., Wirblich, C., Croce, K.R., Schnell, M.J., Jessell, T.M., and Losonczy, A. (2016). Rabies virus CVS-N2c ΔG strain enhances retrograde synaptic transfer and neuronal viability. *Neuron* 89, 711–724.
- Rossi, S.L., Nistor, G., Wyatt, T., Yin, H.Z., Poole, A.J., Weiss, J.H., Gardener, M.J., Dijkstra, S., Fischer, D.F., and Keirstead, H.S. (2010). Histological and functional benefit following transplantation of motor neuron progenitors to the injured rat spinal cord. *PLoS One* 5, e11852.
- Samuels, E., and Szabadi, E. (2008). Functional neuroanatomy of the noradrenergic locus coeruleus: its roles in the regulation of arousal and autonomic function part I: principles of functional organisation. *Curr. Neuropharmacol.* 6, 235–253.
- Takeoka, A., Vollenweider, I., Courtine, G., and Arber, S. (2014). Muscle spindle feedback directs locomotor recovery and circuit reorganization after spinal cord injury. *Cell* 159, 1626–1639.
- Zörner, B., Bachmann, L.C., Filli, L., Kapitzka, S., Gullo, M., Bolliger, M., Starkey, M.L., Röthlisberger, M., Gonzenbach, R.R., and Schwab, M.E. (2014). Chasing central nervous system plasticity: the brainstem's contribution to locomotor recovery in rats with spinal cord injury. *Brain* 137, 1716–1732.

Stem Cell Reports, Volume 8

Supplemental Information

Comprehensive Monosynaptic Rabies Virus Mapping of Host Connectivity with Neural Progenitor Grafts after Spinal Cord Injury

Andrew F. Adler, Corinne Lee-Kubli, Hiromi Kumamaru, Ken Kadoya, and Mark H. Tuszynski

Supplemental Figures

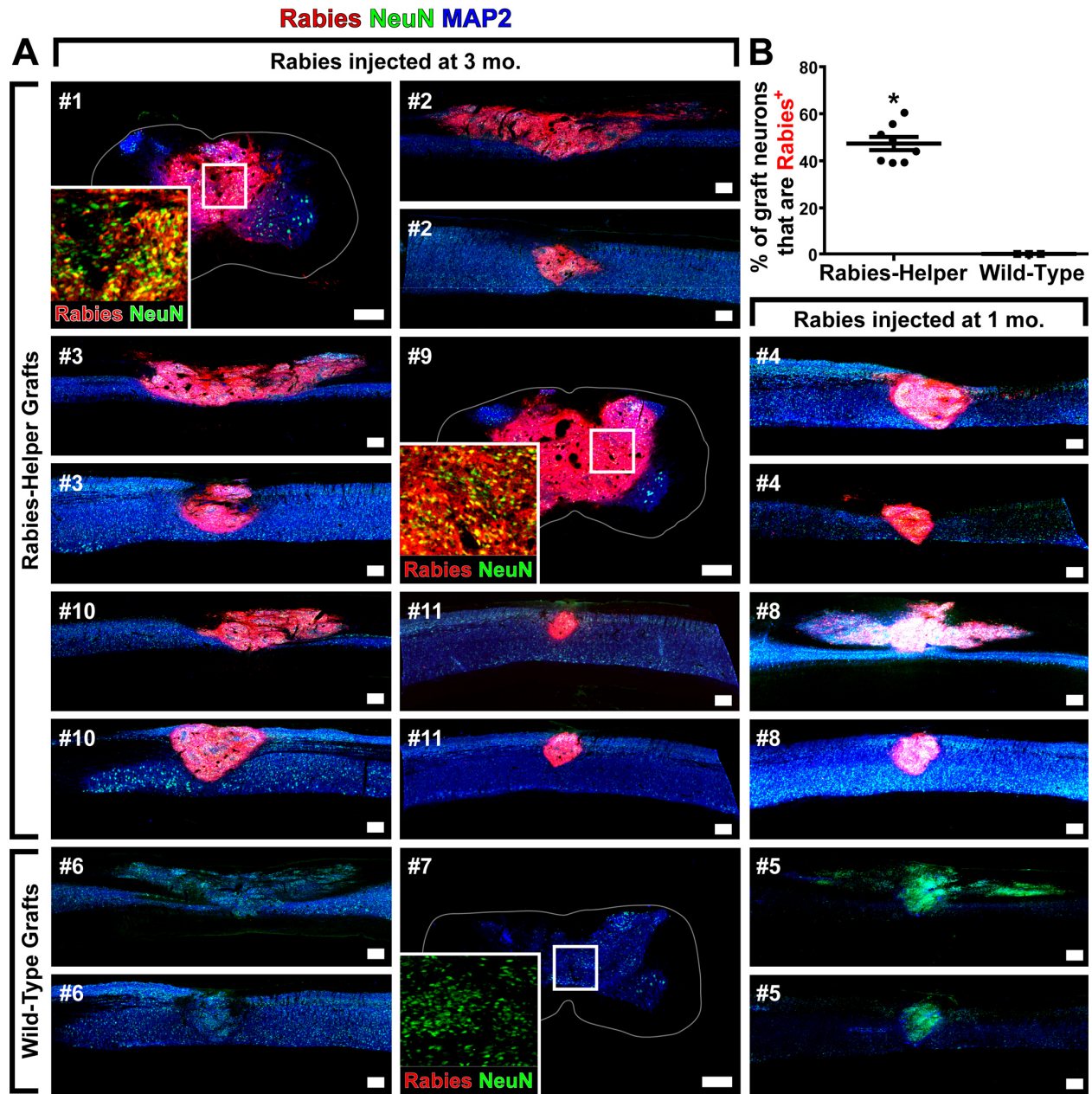


Figure S1. Graft sites of all animals used in these experiments, related to Figure 1. Host mouse identification numbers are indicated in the top left of panels. (A) Sagittal sections (with exception of transverse sections in #1, #7, #9), with rostral to the left, of all E12.5-E13.5 spinal NPC grafts in this study. When possible, a section near the central canal, as well as a more lateral section are provided here to illustrate the extent of the graft sites. All NPC grafts contained NeuN⁺MAP2⁺ neurons after either 1 or 3 months of maturation. Rabies-Helper grafts were infected and expressed EnvA-SADΔG-mCherry rabies virus throughout in all cases, whereas Wild-Type grafts were not infected. White lines denote the extent of white matter for transverse sections. Insets depict detail of boxed regions. Scale bars 250 μm, 30 μm-thick sections. (B) Quantification of the percentage of NeuN⁺ graft neurons that were also mCherry-Rabies⁺ at the end of the experiment (mean ± SEM, n = 8 Rabies-Helper grafts, n = 3 Wild-Type grafts). Asterisk denotes significance by Fisher's exact test of a 2×2 two-tailed contingency table comparing Rabies-Helper and Wild-Type NPC grafts, P < 0.01.

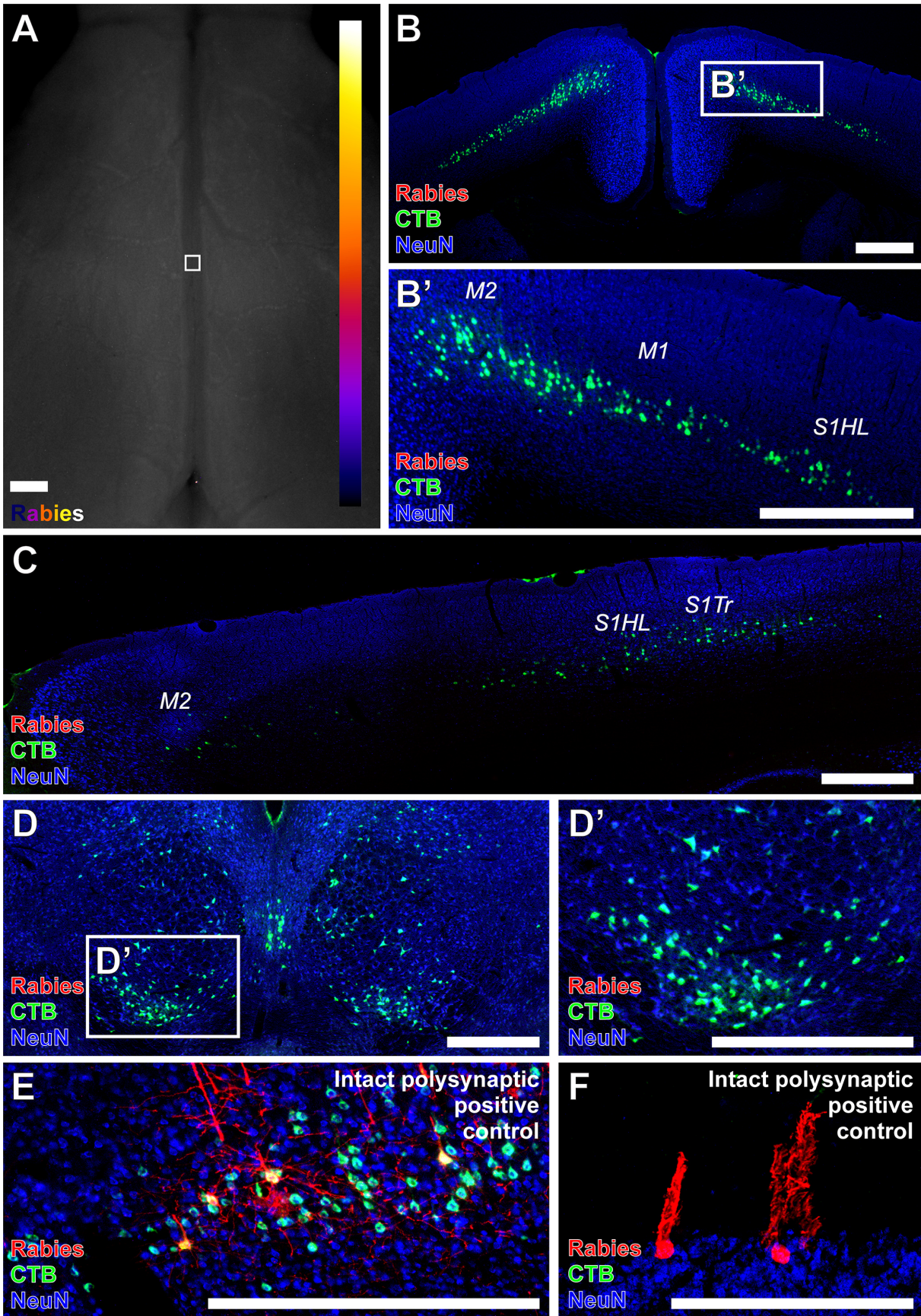


Figure S2. Negative Controls: Brains of hosts grafted with Wild-Type spinal NPCs were not labeled with EnvA-SADΔG-mCherry rabies virus, related to Figure 2. (A-D) Host brain regions in animals co-injected with CTB/EnvA-SADΔG-mCherry rabies virus following Wild-Type NPC grafting were retrogradely labeled with CTB in similar regions to animals receiving Rabies-Helper grafts, but were never labeled with rabies virus. Panels (A-B) and (C-D) correspond to Fig. 2A-B and 2D-E, respectively. Corresponding images were labeled, imaged, and processed identically. **Positive Controls: Brains of intact adult Rabies-Helper animals injected with EnvA-SADΔG-mCherry were extensively labeled with Rabies-mCherry, related to Figure 2.** (E) The M1 cortical section most densely labeled with polysynaptic Rabies-mCherry tracing among intact adult Rabies-Helper animals co-injected at C4 with CTB/EnvA-SADΔG-mCherry rabies virus. (F) Purkinje cells in cerebellar cortex were labeled with polysynaptic Rabies-mCherry tracing in intact adult Rabies-Helper animals, but never in Rabies-Helper grafted animals. Scale bars 500 μm, 30 μm-thick sections. (A) Horizontal, (B, D, E, F) coronal, (C) sagittal views. Abbreviations: M1 primary motor cortex; M2 secondary motor cortex; S1HL primary somatosensory cortex, hindlimb; S1Tr primary somatosensory cortex, trunk.

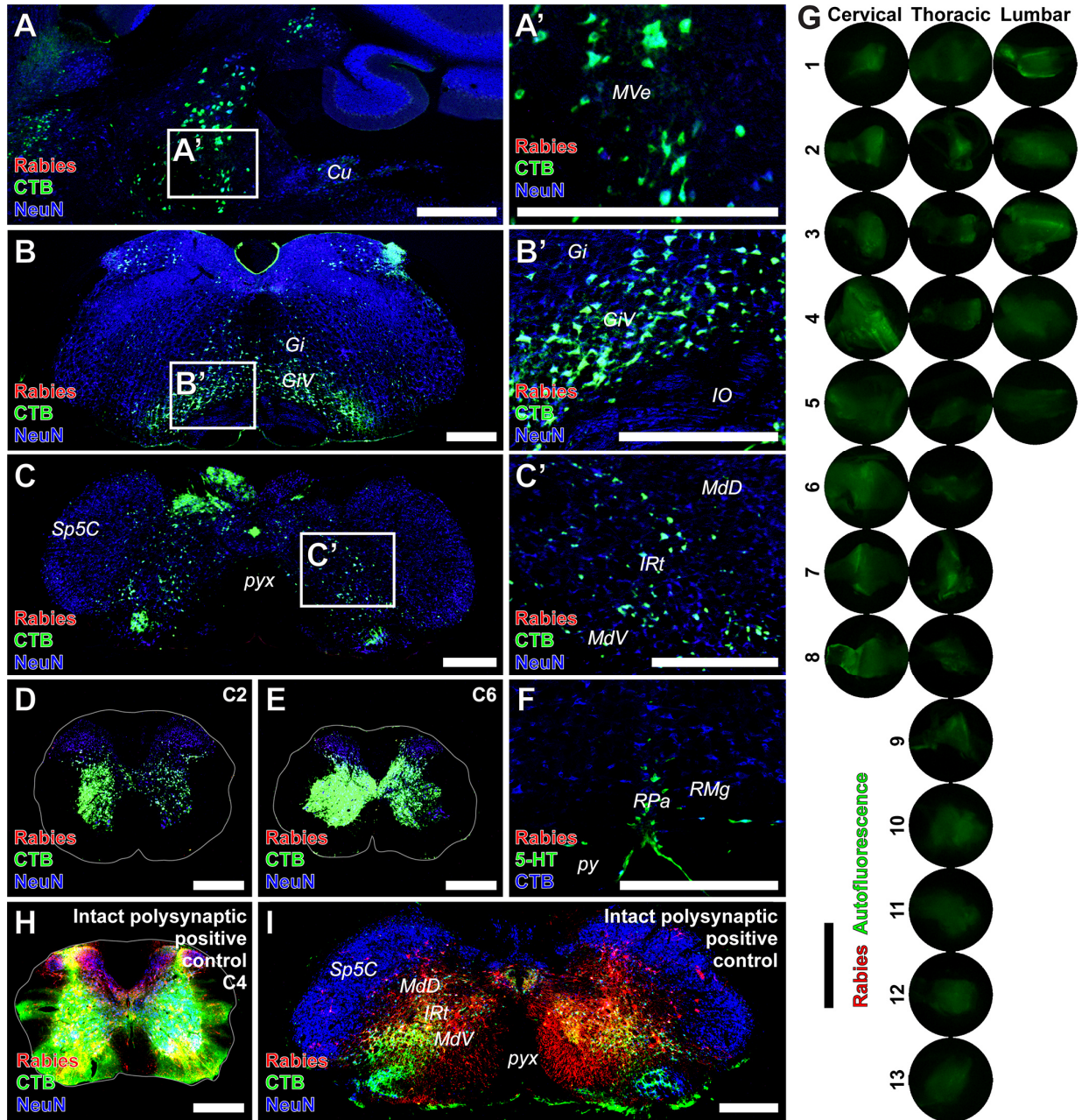


Figure S3. Negative Controls: Brainstems, spinal cords, and dorsal root ganglia of hosts grafted with Wild-Type spinal NPCs were not labeled with EnvA-SADΔG-mCherry rabies virus, related to Figures 3-4. Host brainstem, spinal cord, and dorsal root ganglia in animals co-injected with CTB/EnvA-SADΔG-mCherry rabies virus were retrogradely labeled with CTB in similar regions to animals receiving Rabies-Helper grafts, but were never infected with rabies virus. Panel (A) corresponds to Fig. 3J, (B) to Fig. 3A, (C) to Fig. 3D, (D-E) to Fig. 4A-B, (F) to Fig. 3G, and (G) to Fig. 4G. Corresponding images were stained, imaged, and processed identically to each other. **Positive Controls: (H) Injection sites and (I) brainstems of intact adult Rabies-Helper animals injected with EnvA-SADΔG-mCherry at C4 were extensively labeled with Rabies-mCherry.** Scale bars 500 μm, 30 μm-thick sections. (A) Sagittal view, (B-F, H-I) transverse views. Abbreviations: Gi gigantocellular reticular nu.; GiV gigantocellular reticular nu., ventral part; IO inferior olive, IRt intermediate reticular nu.; MdD medullary reticular nu., dorsal part; MdV medullary reticular nu., ventral part.; MVe medial vestibular nu.; py pyramids; pyx pyramidal decussation; RMg raphe magnus nu.; RPa raphe pallidus nu.; S1 primary somatosensory; Sp5C spinal trigeminal nu..

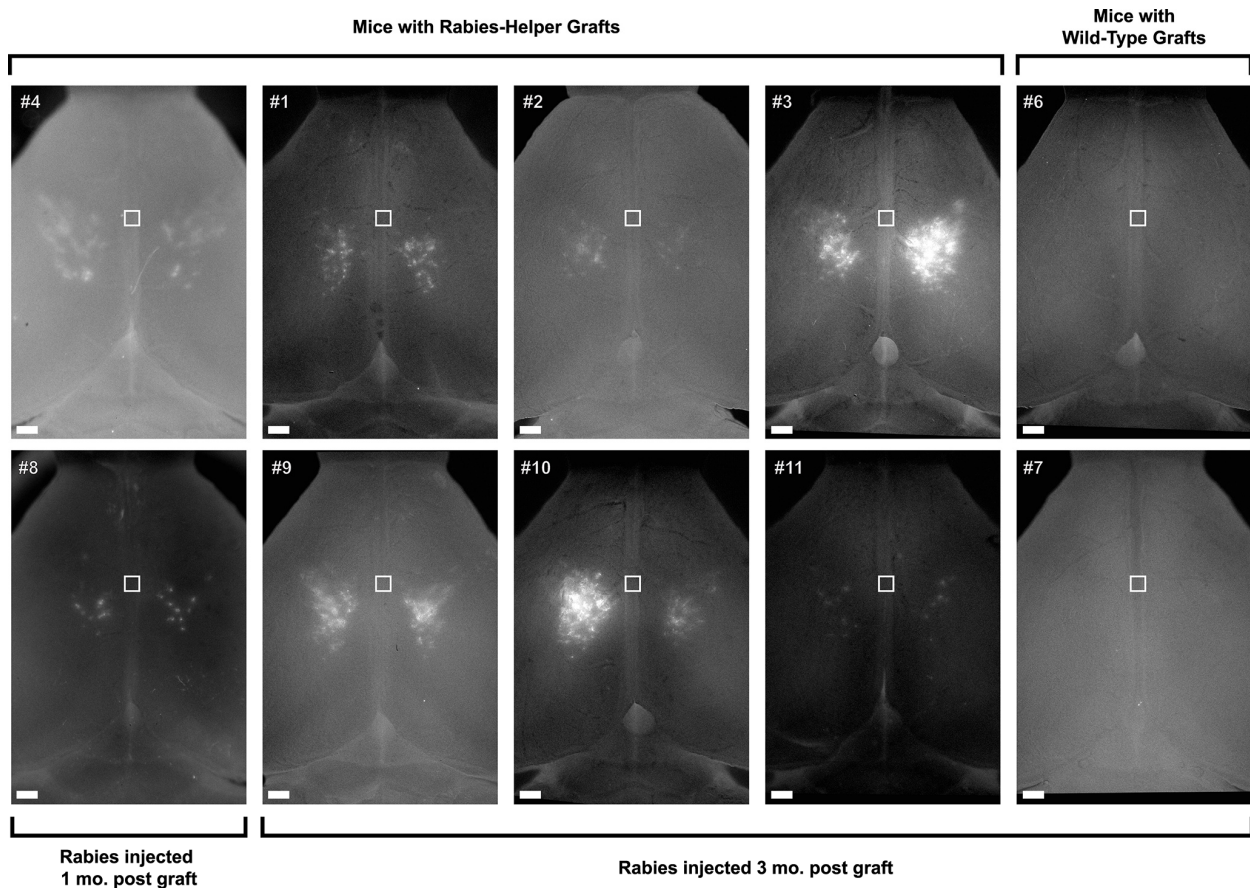


Figure S4. Cortical rabies labeling of individual animals, related to Figures 2A and S2A. Each individual image included in the production of Fig. 2A, and S2A. Corticospinal neurons of host animals receiving Rabies-Helper spinal NPC grafts were consistently transsynaptically labeled in similar regions of the cortex, whereas host animals receiving Wild-Type grafts were not labeled at all. Host mouse identification numbers are indicated in the top left of each panel. Mouse #5 is not depicted, because a gross cortical image was not collected before sectioning the brain; however, no Rabies-mCherry⁺ cells were present in animal #5 upon sectioning. Horizontal views, boxes denote bregma, with rostral at top of images. Scale bars 500 μ m.

RABIES RAW CTB RAW	M1	M2	S1	S2	Red Nucleus	Reticular	Raphe	Vestibular	Other brainstem	TOTAL
Rabies-Helper Grafted #1	88 4688	32 3368	64 3352	8 448	16 1104	318 30228	0 1278	150 2028	210 10938	886 57432
Rabies-Helper Grafted #3	280 1176	136 2328	176 576	16 224	32 1664	438 5760	12 258	66 732	168 1890	1324 14608
Rabies-Helper Grafted #4	64	24	56	0	16	78	6	42	42	328
Rabies-Helper Grafted #8	64	8	16	0	0	48	12	0	42	190
Rabies-Helper Grafted #11	42 1232	12 3152	12 1240	0 912	0 1024	24 9568	6 480	6 1056	30 3168	132 21832
Wild-Type Grafted #5	0	0	0	0	0	0	0	0	0	0
Wild-Type Grafted #6	0 5280	0 7960	0 3104	0 864	0 1368	0 12780	0 576	0 996	0 5904	0 38832
Intact (Poly-synaptic) #1	88 1872	0 680	184 1928	0 128	192 616	3888 15600	408 912	516 1440	1800 9252	7076 32428
Intact (Poly-synaptic) #2	40 3136	0 1064	24 2640	0 240	272 2288	2532 31656	102 1140	288 2820	1422 19164	4680 64148
Intact (Poly-synaptic) #3	8 1264	0 560	8 1376	0 96	72 584	1104 15228	150 576	84 1320	558 6192	1984 27196

% ALL RABIES % ALL CTB	M1	M2	S1	S2	Red Nucleus	Reticular	Raphe	Vestibular	Other brainstem	TOTAL
Rabies-Helper Grafted #1	9.9 8	3.6 6	7.2 6	0.9 1	1.8 2	35.9 53	0.0 2	16.9 4	23.7 19	100.0 100
Rabies-Helper Grafted #3	21.1 8	10.3 16	13.3 4	1.2 2	2.4 11	33.1 39	0.9 2	5.0 5	12.7 13	100.0 100
Rabies-Helper Grafted #4	19.5	7.3	17.1	0.0	4.9	23.8	1.8	12.8	12.8	100.0
Rabies-Helper Grafted #8	33.7	4.2	8.4	0.0	0.0	25.3	6.3	0.0	22.1	100.0
Rabies-Helper Grafted #11	31.8 6	9.1 14	9.1 6	0.0 4	0.0 5	18.2 44	4.5 2	4.5 5	22.7 15	100.0 100
Wild-Type Grafted #5	N/A	N/A	N/A	N/A	N/A	N/A	N/A	N/A	N/A	N/A
Wild-Type Grafted #6	N/A 14	N/A 20	N/A 8	N/A 2	N/A 4	N/A 33	N/A 1	N/A 3	N/A 15	N/A 100
Intact (Poly-synaptic) #1	1.2 6	0.0 2	2.6 6	0.0 0	2.7 2	54.9 48	5.8 3	7.3 4	25.4 29	100.0 100
Intact (Poly-synaptic) #2	0.9 5	0.0 2	0.5 4	0.0 0	5.8 4	54.1 49	2.2 2	6.2 4	30.4 30	100.0 100
Intact (Poly-synaptic) #3	0.4 5	0.0 2	0.4 5	0.0 0	3.6 2	55.6 56	7.6 2	4.2 5	28.1 23	100.0 100
Rabies-Helper Grafted AVG	23.2 ± 4.3 8.9 ± 1.7	6.9 ± 1.3 14.2 ± 3.1	11.0 ± 1.8 5.9 ± 0.8	0.4 ± 0.3 2.2 ± 0.7	1.8 ± 0.9 5.4 ± 2.1	27.2 ± 3.2 42.2 ± 4.1	2.7 ± 1.2 1.9 ± 0.2	7.9 ± 3.1 4.0 ± 0.6	18.8 ± 2.5 15.4 ± 1.3	100.0 100.0
Intact (Poly-synaptic) AVG	0.8 ± 0.2 5.1 ± 0.3	0.0 ± 0.0 1.9 ± 0.1	1.2 ± 0.7 5.0 ± 0.5	0.0 ± 0.0 0.4 ± 0.0	4.1 ± 0.9 2.5 ± 0.5	54.9 ± 0.4 51.1 ± 2.4	5.2 ± 1.6 2.2 ± 0.3	5.9 ± 0.9 4.6 ± 0.1	28.0 ± 1.4 27.1 ± 2.2	100.0 100.0

Table S1. Individual raw counts and percentages relative to total of Rabies-mCherry⁺ neurons in all grafted and adult intact Rabies-Helper animals that were sectioned transversely, related to quantifications in Figures 2 and 3. CTB⁺ neuron counts and distributions are also provided for animals injected after 3 months of graft maturation (Grafted animals #1, #3, #6, #11), and for adult intact Rabies-Helper animals. (The idea to co-inject CTB had not yet been conceived at the time animals with 1 month old grafts were injected with rabies).

Supplemental Experimental Procedures

Mouse breeding

Eighteen adult mice were used (Jackson Laboratory): wild-type (C57BL/6) n = 1, RΦGT (B6;129P2-Gt(ROSA)26Sor^{tm1(CAG-RABVgp4,-TVA)Arenk/J}) n = 2, athymic nude mice (NU/J) n = 12, Rabies-Helper (B6;129P2-Gt(ROSA)26Sor^{tm1(CAG-RABVgp4,-TVA)Arenk/J} × B6.Cg-Tg(Syn1-cre)671Jxm/J) n = 3. Twenty-seven embryonic mice were used: Wild-Type n = 9, Rabies-Helper n = 18. E12.5-E13.5 Rabies-Helper embryos were produced by timed mating of homozygous Syn-Cre sires with homozygous RΦGT dams, ensuring all progeny expressed the helper components.

Spinal cord injury and grafting

During surgery, mice were deeply anesthetized with a combination of acepromazine, xylazine, ketamine, and isoflurane. Laminectomies were performed on athymic nude mice at the fourth cervical vertebral level (C4). A wire knife (McHugh Milieux), which was selected to span from the center of each dorsal horn, was stereotactically inserted, such that the lowest point of the extended knife would be 1.1 mm down from the dorsal surface of the cord. The knife was then raised to lesion the central gray matter, the CST in its entirety, and to partially lesion the ascending sensory fibers, leaving a spared rim of dorsal white matter.

Spinal cords were dissected from E12.5-E13.5 Wild-Type or Rabies-Helper embryos on ice cold HBSS, dissociated with Accutase and gentle trituration, strained through a 70 μm cell strainer, centrifuged for 7 minutes at 300×g, resuspended in DPBS, counted, spun for another 7 minutes at 300×g, decanted, resuspended, and the final volume of concentrated cell suspension was measured with a micropipette. 1M viable spinal NPCs (Trypan Blue exclusion) were grafted immediately after lesion, into the center of lesion sites, in a volume of 2 μL DPBS, using a Picospritzer III (Parker Hannifin) and pulled glass pipettes. A fibrin matrix or growth factor cocktail was not necessary to enable graft survival in this enclosed lesion cavity. After surgery, animals were supported with heat, Neo-Predef, and banamine/ampicillin injections in Lactated Ringer's solution.

EnvA-pseudotyped-SADAG rabies virus/CTB injections

Upon graft maturation, the grafting site was re-exposed, and fibrous scar overlying the dura was gently removed with a scalpel. Small pilot holes were punctured in dura with an insulin syringe, to allow stereotactic insertion of pulled and beveled glass micropipettes, containing 1×10^7 vg/mL EnvA-SADAG-mCherry rabies virus (Salk Institute GT3 Core) in HBSS. Grafts at 3 months of maturation were co-injected with 1×10^7 vg/mL EnvA-SADAG-mCherry rabies virus and 0.2% CTB (List Biological Laboratories) in HBSS. A total of 1.5 μL of viral suspension was injected with a Picospritzer evenly across 8 sites into each graft, at depths of 0.7, 0.5, 0.3 mm at each site, for an infusion of ~ 60 nL/injection, over a period of approximately one hour per animal. Picospritzer pressure and/or pulse duration was adjusted for each pipette to barely overcome capillary forces before insertion, enabling a gentle infusion of viral suspension. Injection sites were balanced as much as overlying vasculature would allow in the rostrocaudal and mediolateral directions for each graft. With exception of Rabies-Helper-grafted mouse #11, control and Rabies-Helper grafts were always injected in the same surgical session, drawing from the same tube of EnvA-SADAG rabies virus or EnvA-SADAG rabies virus/CTB mixture. For adult polysynaptic positive control Rabies-Helper mouse injections, a laminectomy was performed at C4, and a total of 1.5 μL of 1×10^7 vg/mL EnvA-SADAG-mCherry rabies virus and 0.2% CTB suspension was co-injected bilaterally through the center of the dorsal horn, across 8 sites, at depths of 1.1, 0.7, 0.3 mm at each site, for an infusion of ~ 60 nL/injection, over a period of approximately one hour per animal. All animals were sacrificed 7 days after rabies virus injections.

Immunofluorochemistry

Animals were deeply anesthetized with a mixture of ketamine and xylazine, and transcardially perfused with ice-cold phosphate-buffered saline (PBS), then 4% PFA in phosphate-buffered saline. Spinal columns were removed, post-fixed for 24 hours at 4 °C in 4% PFA, then cryoprotected for a minimum of 24 hours in 30% sucrose in PB. The CNS and DRGs were then dissected, and cryoprotected for an additional 24 hours in 30% sucrose in PB. Brains and spinal cords were blocked, frozen, and sectioned at a thickness of 30 µm with a sliding microtome. DRGs were embedded in OCT, and sectioned at a thickness of 20 µm on a cryostat.

For free-floating section immunofluorescence, sections were blocked for 1 hr at room temperature (RT) in blocking buffer (0.2% Triton-X and 10% donkey serum in Tris-buffered saline). Primary antibodies were incubated with sections in blocking buffer overnight at 4 °C, washed, and then incubated with streptavidin or AlexaFluor 488-, 594-, or 647-conjugated secondary antibodies raised in donkey. DRG sections were direct-mounted to subbed slides, and subjected to 30 min of heat-induced antigen retrieval at 80°C in pH 9.0 Tris-HCl buffer before staining on-slide. Primary antibodies used included: Ch α mCherry (EnCor Biotechnology CPCA-mCherry, 1:1000), Ch α MAP2 (EnCor Biotechnology CPCA-MAP2, 1:1000), Gt α mCherry (SICGEN AB0040-200, 1:1000), Gt α CTB (List Labs #703, 1:2500), Rb α NeuN (Biosensis R-3770-100, 1:1000), Rb α 5-HT (Immunostar 20080, 1:2500), Rb α TH (Millipore AB152, 1:1000), Gt α ChAT (Genetex GTX82725, 1:500), Sh α CHX10 (Abcam ab16141, 1:200), Gt α SATB1 (Santa Cruz sc-5989, 1:500), Ch α CALRETININ (EnCor Biotechnology CPCA-CALRETININ, 1:1000), Ch α NF200 (Millipore AB5539, 1:500), Gt α CGRP (Abcam ab36001, 1:1000), biotin-conjugated IB4 (Sigma L2140, 1:500).

Image Analysis

Sections were mounted in Mowiol, and imaged with Olympus AX70 (widefield) or FV-1000 (confocal) fluorescence microscopes. Image window/level were adjusted with ImageJ (FIJI), and long exposures in the far red channel were processed with the “despeckle” command. Comparable regions imaged between Figs. 2-4 and S2-S3 (indicated in caption) were imaged together, with identical acquisition settings and processing in ImageJ. For gross anatomical imaging, autofluorescent background images were captured in the 488 channel, and subtracted from mCherry signal in the 594 channel to produce Figs. 1E, 1J, 2A, 4G, and S2A, S3G, and S4; this background subtraction was performed equivalently for all samples. For quantification of Rabies-mCherry⁺ neurons in Figs. 2-3, all neurons in every 6th (8th) section through brainstem (cortex) were manually counted for all animals cut transversely (#1, 3, 4, 8, 11 Rabies-Helper, and #5, 6 Wild-Type) from olfactory bulb to the pyramidal decussation. No significant differences in the ratio of host labeling were detectable between animals injected with rabies at 1 or 3 months following injury and engraftment, so their counts were pooled. Counter was blinded to experimental conditions for the determination of whether any Rabies-mCherry⁺ cells were observed in control animals during quantifications performed for Figs. 2-4 (none were observed). ImageJ macros were used to count polysynaptic mCherry⁺ neurons, CTB⁺ neurons, and mCherry⁺NeuN⁺ graft neurons (Fig. S1B) in an automated fashion. ImageJ macros set a local threshold of a defined radius around each pixel, excluded masked objects that were too large or small to be neurons, and then counted the remainder within ROIs defined with the aid of an atlas of the mouse brain.